

# Raman Microspectroscopy of Thienothiadiazole-Fluorene Copolymer and its Blends with Fullerene

Zuzana Morávková, Veronika Pokorná, Drahomír Výprachtický, Ivan Kmínek, Vera. Cimrová\*

**Summary:** Thin films made of a low-band gap copolymer poly{4,6-bis-(3-dodecylthien-2-yl)thieno[3,4-c][1,2,5]thiadiazole-*alt*-9,9-bis(2-ethylhexyl)-fluorene} (CDTF) and made of its blends with soluble fullerene derivative [6,6]-phenyl C61-butyric acid methyl ester (PCBM60) with various ratios were studied by means of UV–vis absorption spectroscopy and Raman microspectroscopy. It was found that inhomogeneities which are present in thin films consist of higher content of PCBM60 than the rest of the film. Photoluminescence of both components observed in the Raman spectra was distinguished using two different excitation wavelengths.

**Keywords:** bulk heterojunction; conjugated polymers; low-band gap; Raman spectroscopy; UV–vis spectroscopy

## Introduction

Low-band gap copolymers and their blends with fullerenes are intensively studied because they can be used as active layers in organic photovoltaic devices (PV). PV devices made of donor-acceptor blends with bulk heterojunction belong to the most promising.<sup>[1–3]</sup> Recently, we have prepared a novel series of low-band gap copolymers with electron accepting thienothiadiazole-based units, which are promising for photovoltaic applications due to the low-band gap, high electron affinity and reversible redox properties.<sup>[4–9]</sup> The quality of the blend film is important for the PV device performance.<sup>[10–13]</sup> Raman spectroscopy is a useful tool to monitor local polymer order and particularly, Raman microspectroscopy enable us to study the chemical composition of blends used in bulk-heterojunction structure.<sup>[11–16]</sup>

In this paper, we present a study of thin films made of the low-band gap copolymer poly{4,6-bis(3-dodecylthien-2-yl)thieno[3,4-c][1,2,5]thiadiazole-*alt*-9,9-bis(2-ethyl-hexyl)

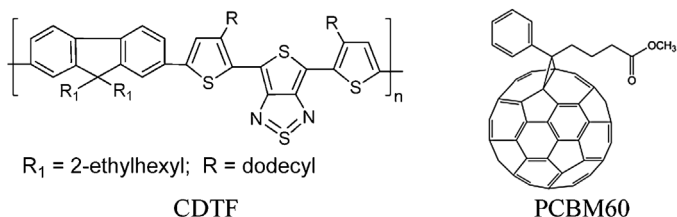
fluorene} (CDTF) and its blends with soluble fullerene derivative [6,6]-phenyl C61-butyric acid methyl ester (PCBM60) with various ratios by means of UV–vis absorption spectroscopy and Raman microspectroscopy. The Raman measurements were performed at two different excitation wavelengths (633 nm and 785 nm) to distinguish low-wavelength photoluminescence (PL) of both components. Chemical structure of the materials under study is shown in Figure 1.

## Experimental Part

### Materials and Thin Film Preparation

Copolymer CDTF was prepared by the Suzuki coupling reaction of 9,9-bis(2-ethyl-hexyl)-2,7-bis(1,3,2-dioxaborinan-2-yl)fluorene with 4,6-bis(5-bromo-3-dodecylthien-2-yl)thieno[3,4-c][1,2,5]thiadiazole. The details of the synthesis are described in our previous paper.<sup>[7]</sup> The molecular weight was  $M_n = 31000$  and  $M_w = 42000$ . Thin polymer and polymer blends films were prepared by spin-coating. All films were spin-coated from 1,2-dichlorobenzene solutions, which were filtered with 0.45  $\mu\text{m}$  Millex-FH<sub>13</sub> Millipore syringe filters prior to spin-coating. Thin films for UV–vis studies were prepared

Institute of Macromolecular Chemistry, Academy of Sciences of the Czech Republic, Czech Republic  
E-mail: cimrova@imc.cas.cz

**Figure 1.**

Chemical structure of poly{4,6-bis(3-dodecylthien-2-yl)thieno[3,4-c][1,2,5]thiadiazole-*alt*-9,9-bis(2-ethylhexyl)fluorene} (CDTF) and [6,6]-phenyl C61-butyric acid methyl ester (PCBM60).

onto fused silica substrates and for Raman microspectroscopic measurements onto silicon (Si) substrates. All films were dried in vacuum ( $10^{-3}$  Pa) at 353 K for 2 h. All thin film preparations were done in glove box under nitrogen atmosphere.

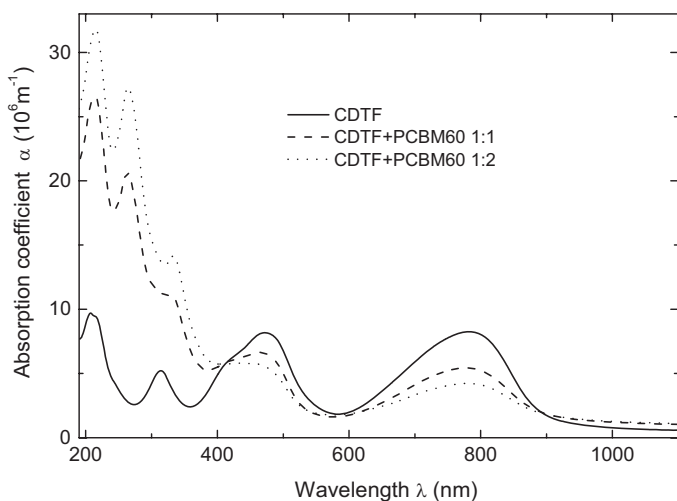
### Measurements

Layer thicknesses were measured using a KLA-Tencor P-10 profilometer. UV-vis spectra were recorded using a Perkin-Elmer Lambda 35 UV-vis spectrometer. Raman spectra were measured on an InVia Reflex Renishaw microspectrometer using excitation lasers with wavelengths 633 and 785 nm at various spots in the films. The laser power was set for each laser to a maximal value at which the fluorescence of all the samples did not cause an overflow on

the detector (cca 0.5 mW for 633 nm and 0.01 mW for 785 nm). The optical images were taken on a Leica optical microscope attached to the Raman microspectrometer. Raman spectra were measured with the magnification of 50.

### Results and Discussion

UV-vis absorption spectra of the CDTF thin film and thin films made of its blends with PCBM60 with various concentrations are shown in Figure 2. In absorption of CDTF films low-energy absorption bands with maxima at 473 nm and at 780 nm were observed, which are assigned to the lowest  $\pi - \pi^*$  transition and to the intrachain charge-transfer (ICT) transition, respectively. PCBM60 absorbs in the UV spectral

**Figure 2.**

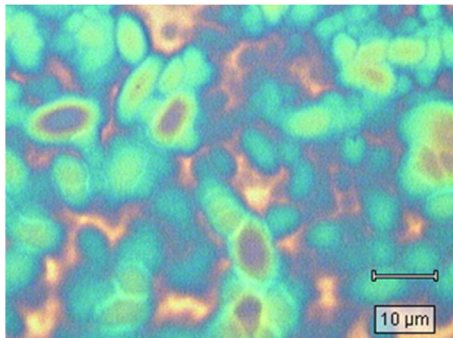
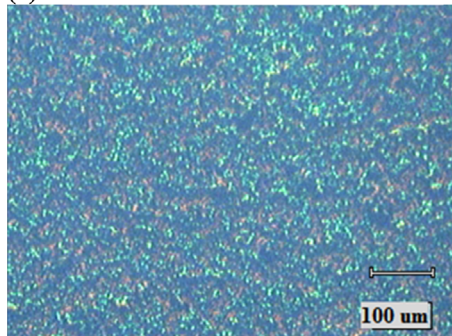
UV-vis absorption spectra of the CDTF thin film (solid) with a thickness  $d = 76$  nm, and thin films of its blends CDTF + PCBM60 with CDTF:PCBM60 ratios 1:1 (dashed;  $d = 114$  nm) and 1:2 (dotted;  $d = 109$  nm).

region therefore in the blend films depending on the PCBM60 content the UV absorption increased and absorption in the visible region decreased compared with the absorption of CDTF neat thin film. No significant shifts in the maxima positions were detected after blending. It indicates that blending CDTF with PCBM60 does not hinder planarization of the main chain, i.e. does not influence ICT, and it also does not prevent strong intermolecular interac-

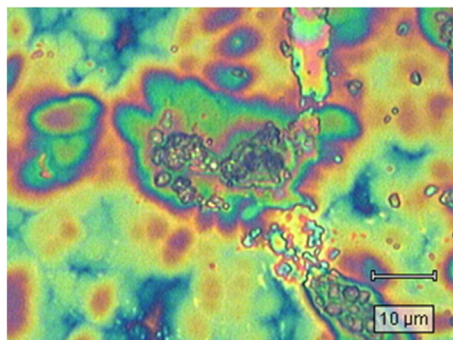
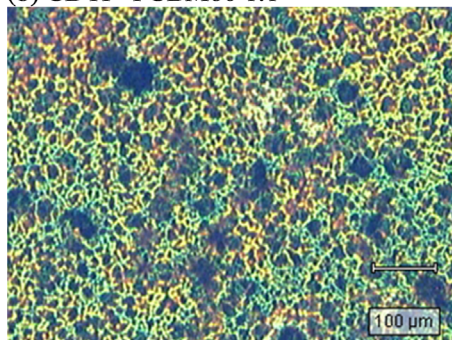
tions between polymer chains leading to the aggregate formation in thin films. The strong aggregation in the CDTF thin films was shown in our previous papers<sup>[6,7]</sup> from the comparison of absorption in solution and thin films. In thin film absorption spectra the low-energy absorption maxima are significantly red-shifted compared to those in its solution spectra.

Figure 3 shows optical microscopic pictures of thin CDTF films and CDTF +

(a) CDTF



(b) CDTF+PCBM60 1:1



(c) CDTF+PCBM60 1:2

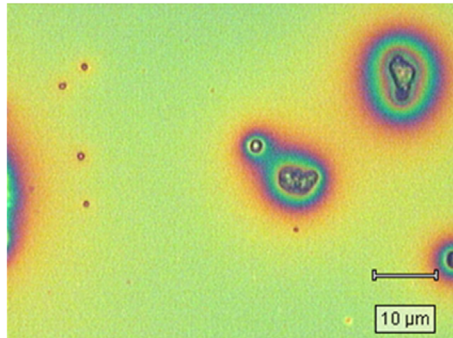
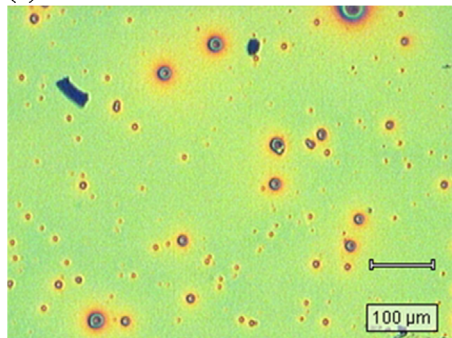


**Figure 3.**

Optical microscopic pictures of thin CDTF films (a) and CDTF + PCBM60 blend films with CDTF:PCBM60 ratios (b) 1:1 and (c) 1:2.

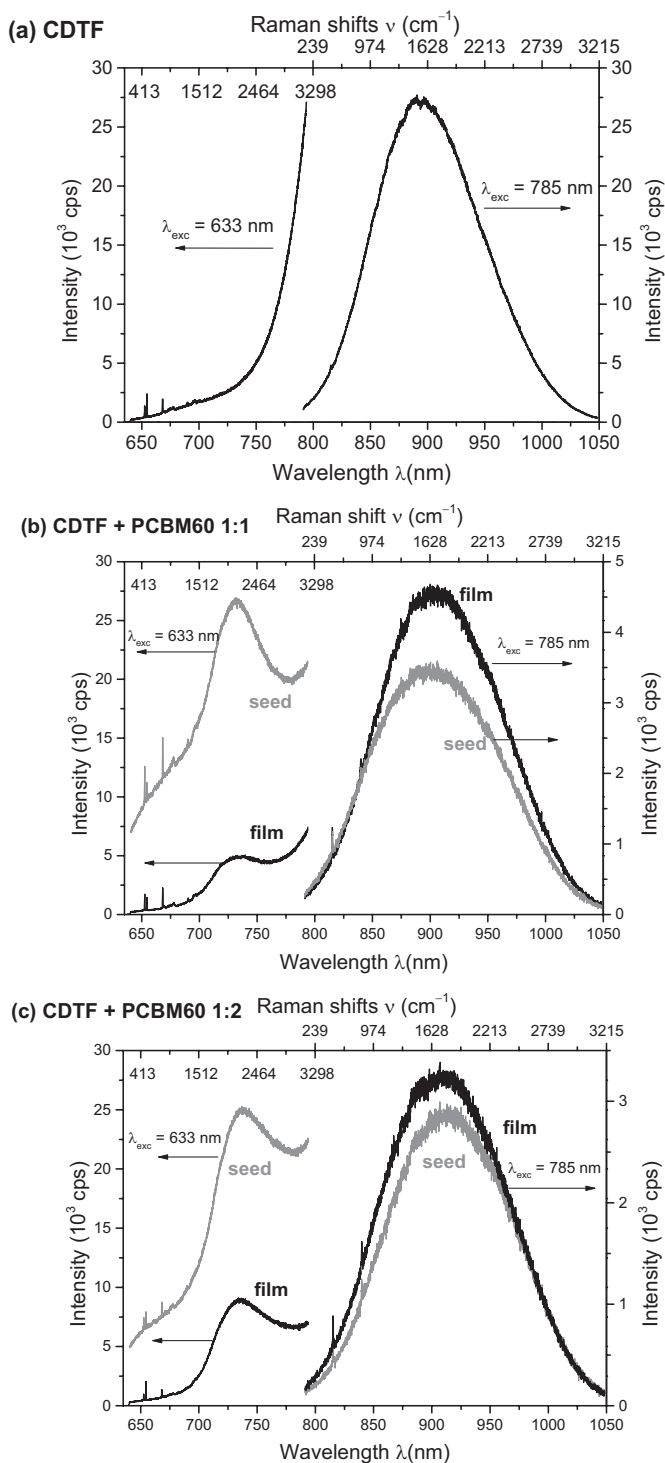


**Figure 4.**

Raman-photoluminescent emission spectra of (a) CDTF film and CDTF + PCBM60 blend films with CDTF:PCBM60 ratios: (b) 1:1 and (c) 1:2 measured with excitation 633 nm and 785 nm in different spots (film and seeds).

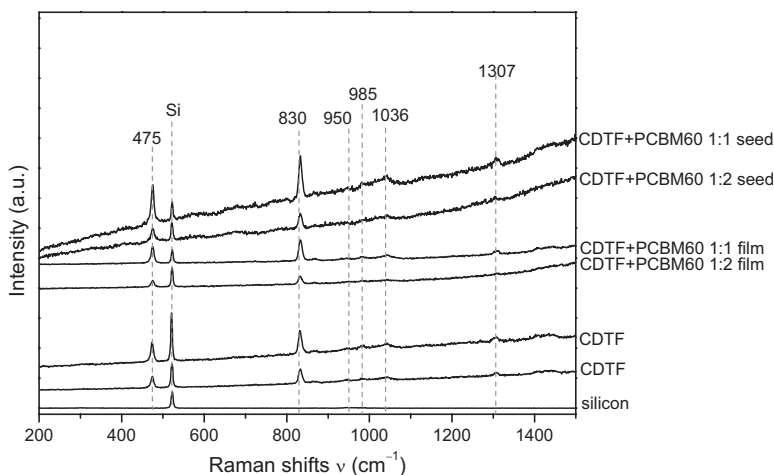


**Figure 5.**

Raman spectra of CDTF film and CDTF + PCBM60 blend films with CDTF:PCBM60 ratios 1:1 and 1:2 measured at various areas (laser excitation at 633 nm).

PCBM60 blend films with CDTF:PCBM60 ratios 1:1 and 1:2, indicating inhomogeneity in the blend films. The components are not homogeneously spread in all blend films. Separated areas (seeds), several up to tens of micrometers large, were observed by optical microscopy. We used Raman microspectroscopy to study the inhomogeneity's composition. The both components of the blends exhibited photoluminescence therefore two laser wavelength (633 nm and 785 nm) were used for excitation. Raman spectra were measured both on homogeneous areas and on seeds. The spectra are displayed in Figure 4.

A weak PL was observed in Raman spectra. In the neat CDTF thin film spectrum a broad-band PL with a maximum at about 890 nm prevailed for the excitation wavelength of 785 nm (see Figure 4a). In the blend film spectra measured with the 633 nm excitation PL emission with a maximum at about 730 nm was observed, which can be assigned to the PCBM60 emission.<sup>[17]</sup> The spectra of the seed visible in the optical micrographs and the rest of the film differ in the PL intensity of the individual components. In the seed, the PL emission intensity of CDTF was weaker and the PL intensity of PCBM60 was stronger

than in the rest of the film indicating higher PCBM60 concentration in the seeds (see Figure 4b, c).

Figure 5 shows the details of Raman spectra in the spectral area below 1500  $\text{cm}^{-1}$  measured with 633 nm excitation laser, in which Raman bands of the CDTF polymer are observed at 475  $\text{cm}^{-1}$  corresponding to the skeletal vibration of the fluorene unit, at 830  $\text{cm}^{-1}$  assigned to N–S–N stretching in the thiazole units, at 950  $\text{cm}^{-1}$  skeletal vibration of the fluorene unit, at 985 and 1036  $\text{cm}^{-1}$  thiophene ring vibration, and 1307  $\text{cm}^{-1}$  fluorene unit skeletal vibration.<sup>[18]</sup> Neither their positions nor relative intensities change with the PCBM60 content or between the seeds and the rest of the film. This supports that the blending does not hinder polymer molecule planarization and also does not hinder aggregation due to the strong intermolecular interactions. The peak at 521  $\text{cm}^{-1}$  belongs to the silicon substrate, its intensity correlates with the thickness of the film.

## Conclusion

Optical and Raman spectroscopic study of thin films of low-band gap copolymer

CDTF and of its blends made of CDTF and PCBM60 were performed. Separated areas (seeds), several up to tens of micrometres large, were observed in the blend films indicating that the materials were not homogeneously spread. Photoluminescence of both components was detected in the Raman spectra. It was found out that the seeds contained a higher amount of PCBM60 and a lower amount of the copolymer CDTF compared with the homogeneous blend films. The results indicate that blending CDTF with PCBM60 does not hinder planarization of CDTF backbone and also does not prevent aggregation of polymer chains.

**Acknowledgments:** The authors thank the Grant Agency of the Czech Republic (grants No. 13-26542S and No. P106/12/0827) for financial support.

- [1] a) B. C. Thompson, J. M. J. Frechet, *J. Angew. Chem. Int. Ed. Engl.* **2008**, 47, 58; b) Y.-J. Cheng, S.-H. Yang, C.-S. Hsu, *Chem. Rev.* **2009**, 109, 5868.
- [2] A. J. Heeger, *Chem. Soc. Rev.* **2010**, 39, 2354.
- [3] M. C. Scharber, N. S. Sariciftci, *Progress in Polymer Science* **2013**, 38, 1929.
- [4] V. Cimrová, I. Kmínek, *Macromol. Symp.* **2010**, 295, 65.
- [5] I. Kmínek, V. Cimrová, D. Výprachtický, P. Pavlačková, *Macromol. Symp.* **2008**, 268, 100.
- [6] V. Cimrová, I. Kmínek, D. Výprachtický, *Macromol. Symp.* **2010**, 295, 65.
- [7] I. Kmínek, D. Výprachtický, J. Kříž, J. Dybal, V. Cimrová, *J. Polym. Sci., Part A: Polym. Chem.* **2010**, 48, 2743.
- [8] V. Cimrová, I. Kmínek, P. Pavlačková, D. Výprachtický, *J. Polym. Sci. Part A: Polym. Chem.* **2011**, 49, 3426.
- [9] V. Cimrová, I. Kmínek, P. Pavlačková, D. Výprachtický, *ECS Trans.* **2011**, 33, 119.
- [10] J. Čermák, B. Rezek, V. Cimrová, A. Fejfar, A. Purkrt, M. Vaněček, J. Kočka, *Thin Solid Films* **2010**, 519, 836.
- [11] J. Čermák, B. Rezek, V. Cimrová, D. Výprachtický, M. Ledinský, T. Mates, A. Fejfar, J. Kočka, *Phys. Status Solidi RRL* **2007**, 1, 193.
- [12] J. Čermák, B. Rezek, V. Cimrová, D. Výprachtický, H.-H. Hoerhold, M. Ledinský, A. Fejfar, *Phys. Status Solidi B* **2009**, 246, 2828.
- [13] B. Rezek, J. Čermák, A. Kromka, M. Ledinský, P. Hubík, J. Mareš, A. Purkrt, V. Cimrová, A. Fejfar, J. Kočka, *Nanoscale Res. Lett.* **2011**, 6:238, 1.
- [14] J.-J. Yun, J. Peet, N.-S. Cho, G. C. Bazan, S. J. Lee, M. Moskovits, *Appl. Phys. Lett.* **2008**, 92, 251912–1.
- [15] C. Carach, I. Riisness, M. J. Gordon, *Appl. Phys. Lett.* **2012**, 101, 083302–1.
- [16] S. Falke, P. Eravuchira, A. Materny, C. Lienau, *J. Raman Spectrosc.* **2011**, 42, 1897.
- [17] S.-K. Lin, L.-L. Shiu, K.-M. Chien, T.-Y. Luh, T.-I. Lin, *J. Phys. Chem.* **1995**, 99, 105.
- [18] a) G. Bruno, M. Almeida, D. Simão, M. L. Mercuri, L. Piliá, A. Serpe, P. Deplano, *Dalton Trans.* **2009**, 495; b) L. Cuff, M. Kertesz, *Macromolecules* **1994**, 27, 762; c) V. Hernandez, J. Casado, Y. Kanemitsu, J. T. L. Navarrete, *J. Chem. Phys.* **1999**, 110, 6907; d) J.-S. Kim, P. K. H. Ho, C. E. Murphy, R. H. Friend, *Macromolecules* **2004**, 37, 2861.